Pharm Res (2010) 27:2384–2393
DOI 10.1007/s11095-010-0221-8

RESEARCH PAPER

Influence of Crystallizing and Non-crystallizing Cosolutes on Trehalose Crystallization During Freeze-Drying

Prakash Sundaramurthi • Raj Suryanarayanan

Received: 14 April 2010 / Accepted: 12 July 2010 / Published online: 8 September 2010
© Springer Science+Business Media, LLC 2010

ABSTRACT

Purpose To study the influence of crystallizing and non-crystallizing cosolutes on the crystallization behavior of trehalose in frozen solutions and to monitor the phase behavior of trehalose dihydrate and mannitol hemihydrate during drying.

Methods Trehalose (a lyoprotectant) and mannitol (a bulking agent) are widely used as excipients in freeze-dried formulations. Using differential scanning calorimetry (DSC) and X-ray diffractometry (XRD), the crystallization behavior of trehalose in the presence of (i) a crystallizing (mannitol), (ii) a non-crystallizing (sucrose) solute and (iii) a combination of mannitol and a model protein (lactose dehydrogenase, catalase, or lysozyme) was evaluated. By performing the entire freeze-drying cycle in the sample chamber of the XRD, the phase behavior of trehalose and mannitol were simultaneously monitored.

Results When an aqueous solution containing trehalose (4% *w/v*) and mannitol (2% *w/v*) was cooled to −40°C at 0.5°C/min, hexagonal ice was the only crystalline phase. However, upon warming the sample to the annealing temperature (−18°C), crystallization of mannitol hemihydrate was readily evident. After 3 h of annealing, the characteristic XRD peaks of trehalose dihydrate were also observed. The DSC heating curve of frozen and annealed solution showed two overlapping endotherms, attributed by XRD to the sequential melting of trehalose dihydrate—ice and mannitol hemihydrate—ice eutectics, followed by ice melting. While mannitol facilitated trehalose dihydrate crystallization, sucrose completely inhibited it. In the presence of protein (2 mg/ml), trehalose crystallization required a longer annealing time. When the freeze-drying was performed in the sample chamber of the diffractometer, drying induced the dehydration of trehalose dihydrate to amorphous anhydrate. However, the final lyophiles prepared in the laboratory lyophilizer contained trehalose dihydrate and mannitol hemihydrate.

Conclusions Using XRD and DSC, the sequential crystallization of ice, mannitol hemihydrate, and trehalose dihydrate was observed in frozen solutions. Mannitol, by readily crystallizing as a hemihydrate, accelerated trehalose dihydrate crystallization in frozen solutions. However, by remaining amorphous, sucrose completely inhibited trehalose dihydrate crystallization. Crystallization of the lyoprotectantt in the model protein formulations might have serious implications on protein stability.

KEY WORDS dehydration · DSC · mannitol hemihydrate · processing · protein · trehalose dihydrate · XRD

INTRODUCTION

In addition to the active pharmaceutical ingredient (API), lyophilized formulations often contain a bulking agent, lyoprotectant, buffer and surfactant (1,2). These excipients are incorporated to exert specific functions, wherein their desired physical form, both during processing and in the final product, can potentially influence the product stability and hence the performance (3–6). Crystallization of bulking agents is desirable, both from processing and product-elegance perspectives (7,8). Bulking agents such as mannitol and glycine, when crystallized, enable primary drying at a

P. Sundaramurthi · R. Suryanarayanan (✉)
Department of Pharmaceutics, College of Pharmacy
University of Minnesota
Minneapolis, Minnesota 55455, USA
e-mail: surya001@umn.edu

Present Address:
P. Sundaramurthi
Scientific Affairs, Teva Parenteral Medicines Inc.
17 Hughes
Irvine, California 92618, USA

relatively high temperature and provide a robust matrix during freeze-drying (7–11).

In contrast, crystallization of buffer components and lyoprotectant, an excipient intended to stabilize macromolecules, is undesirable (12–15). Buffer component crystallization in frozen solutions can cause a significant shift in the freeze-concentrate pH. Lyoprotectant crystallization reduces its effectiveness (16,17). The physical state of an excipient not only determines its own functionality, but can also influence the solid state of other solutes including the API (6). For example, crystallization of glycine enhanced the crystallization of sodium phosphate buffer in frozen solutions. In contrast, sucrose, an amorphous solute, completely inhibited buffer crystallization (18,19).

Non-reducing sugars, such as sucrose and trehalose, are widely used as lyoprotectants due to their ability to vitrify during freeze-drying. The high viscosity of the sugar solution in the freeze-concentrate is implicated in their resistance to crystallization. While there are no reports on sucrose crystallization, we recently reported the crystallization of trehalose in frozen solutions (12,13,20,21). Raffinose, a trisachharide consisting of glucose, fructose and galactose readily crystallized in frozen solutions (22–25). At −25°C, the viscosity values of aqueous sucrose, trehalose and raffinose solutions are respectively ~100, 680 and 715 Pa s (26–28). It is clear that viscosity cannot explain the ability of sucrose to resist crystallization. Both trehalose and raffinose crystallize as hydrates, the former as a dihydrate and the latter as a pentahydrate. Obviously the solubility of these hydrates is lower than that of the corresponding anhydrous forms. In addition, the structure in solution could explain the differences in crystallization propensity.

While analyzing the crystal structures of sugars, including sucrose, trehalose and lactose, Jeffrey reported the existence of intramolecular hydrogen bonding in all the disaccharides but trehalose (29–31). The most common intramolecular hydrogen bonding was the linkage between the oxygen (O–2 and O–3′) atoms of the monosaccharide residues (32). Similar intramolecular hydrogen bonds are also absent in raffinose pentahydrate (33). However, in the hydrated crystal form of trehalose or raffinose, it is common to find that two oxygen atoms (O–6 and O–6′) in the monosaccharide residues are linked by hydrogen bonds to water molecules (33–35). The mobility of the fructose moiety in sucrose enables effective hydrogen bonding (intramolecular) with glucose. While investigating the associations of sucrose molecules in aqueous solutions, Mathlouthi *et al.* indicated that the number of intramolecular hydrogen bonds depended on concentration (36). In dilute solutions (10% *w/v*), there was no intramolecular hydrogen bonding, whereas at high sucrose concentrations (82% *w/v*), two bonds are formed between the monosaccharide units. Because of this intramolecular hydrogen bonding and the flexibility of the glycosidic linkage, the torsion angle between the two monosaccharides (glucopyranose and fructofuranose) is less obtuse (114°) than in trehalose dihydrate (116°), cyclohexaamylose (119°) and raffinose (122°) (32). The resistance to crystallization in frozen sucrose solutions could be attributed to the flexibility of the glycosidic linkage and the geometrical constraint imposed by intramolecular hydrogen bonding (36). The inability of trehalose and raffinose to form intramolecular hydrogen bonds can explain their ability to interact with water and crystallize as hydrates (20–25).

While crystallization of raffinose pentahydrate has been extensively reported (22–25), annealing-induced crystallization of trehalose dihydrate in frozen solutions was demonstrated only recently (20,21). In the previous work, aqueous solutions containing only trehalose were investigated. However, freeze-dried pharmaceutical formulations are often multi-component systems. Thus, we wish to determine the influence of crystallizing and non-crystallizing cosolutes on the crystallization behavior of trehalose in frozen solutions. Our hypothesis is that the crystallization of solutes in frozen solutions will facilitate trehalose crystallization. In contrast, a non-crystallizing solute such as sucrose will inhibit trehalose crystallization.

Thus, our objective is to investigate individually the influence of a readily crystallizing (mannitol) and a non-crystallizing (sucrose) cosolute on the crystallization behavior of trehalose in frozen solutions. The effect of model proteins—lactic acid dehydrogenase, glucose oxidase, catalase, and lysozyme—on trehalose crystallization was also evaluated. Both calorimetry and diffractometry were utilized to characterize frozen systems. In an effort to monitor the phase behavior of trehalose dihydrate during drying, the entire freeze-drying cycle was performed in the sample chamber of an X-ray diffractometer.

MATERIALS AND METHODS

Materials

Trehalose dihydrate ($C_{12}H_{22}O_{11}\cdot 2H_2O$), sucrose ($C_{12}H_{22}O_{11}$), mannitol ($C_6H_{14}O_6$), glycine ($C_2H_5NO_2$), L-lactic dehydydrogenase (Type XI: from rabbit muscle; 796 units/mg), glucose oxidase (Type X-S: from Aspergillus niger; 158 units/mg), catalase (from bovine liver; 13,000 units/mg), and lysozyme (from chicken egg white; 58,100 units/mg) were purchased from Sigma and used without further purification. All the solutions were prepared with degassed deionized water. The deionized water was degassed by holding at 70°C for 5 min and filtered through 0.45 μm PTFE membrane filter. The degassed water, stored in a closed container at room temperature (RT), was

used to prepare the solutions. As shown in Fig. 1, prelyo solutions containing a) trehalose (4% *w/v*) and mannitol (2 to 8% *w/v*), b) trehalose (4% *w/v*), mannitol (2% *w/v*) and protein (2 mg/ml), and c) trehalose (4% *w/v*) and sucrose (2 to 8% *w/v*) were investigated.

Methods

X-ray Diffractometry (XRD)

A powder X-ray diffractometer (Model XDS 2000, Scintag; Bragg-Brentano focusing geometry) with a variable temperature stage (High-Tran Cooling System, Micristar, Model 828D, R.G. Hansen & Associates; working temperature range: −190 to 300°C) and a solid-state detector was used. About 1 mL of the aqueous solution was placed into a custom-designed sample holder and hermetically sealed with a stainless steel dome with a beryllium window. Typically, the solutions were cooled from RT to −40°C at 1°C/min, held for 15 min, and then heated at 1°C/min to the annealing temperature of −18°C. When phase quantification was desired, the integrated intensities of the characteristic peaks were obtained. The specific experimental details are provided in the figure legends.

Following the annealing step, primary drying was conducted at −25°C under reduced pressure (150 mTorr). The secondary drying was performed by increasing the temperature, first to −10°C and then to 0°C and finally to +10°C. The frozen mass was periodically exposed to Cu Kα radiation (45 kV × 40 mA) in the reflection mode, and the XRD patterns were obtained using a zero dimensional (point) detector. The samples were scanned over an angular range of 5 to 35° 2θ with a step size of 0.05° and a dwell time of 1 s. The results were compared with the published data in the Powder Diffraction Files (PDF) of the International Centre for Diffraction Data (ICDD) (37).

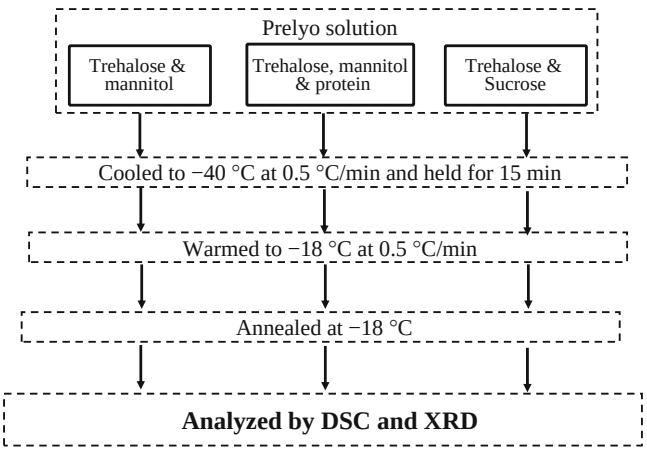

Fig. 1 Schematic representation of the experimental protocol and the systems investigated.

The final lyophiles were analyzed using a powder X-ray diffractometer (Bruker D8 Advance, Bruker AXS, Madison, WI) with Cu Kα radiation (40 kv × 40 mA) and LynxEye™ detector. The diffraction patterns were recorded in the range of 5 to 35° 2θ with a step size of 0.05° and a count time of 1 s.

Differential Scanning Calorimetry (DSC)

A differential scanning calorimeter (MDSC, Model 2920, TA instruments, New Castle, DE) equipped with a refrigerated cooling accessory was used. The instrument was periodically calibrated with tin and indium. About 40–50 mg of aqueous trehalose solution was weighed in an open aluminum pan and cooled from RT to −70°C at 1°C/min. Dry nitrogen at 50 ml/min was used as the purge gas. The frozen solutions were warmed to −18°C at 1°C/min and annealed for 48 h. The annealed samples were then cooled back to −50°C and rewarmed to RT at 1°C/min.

Lyophilization

Trehalose (4% *w/v*) solution was prepared by dissolving the appropriate amount of trehalose dihydrate in water. Trehalose solutions were also prepared containing either sucrose (a non-crystallizing cosolute) or mannitol (a crystallizing cosolute). About 5 ml of the prelyophilization solution was filled into glass vials and then loaded into a bench-top (VirTis® AdVantage™, Gardiner, NY) freeze-dryer. USP Type I borosilicate glass vials (VWR®), with 20 mm neck size and 10 ml fill volume capacity were used. The freeze-dryer shelf was cooled to −40°C at 0.5°C/min, held for 1 h, then heated to −18°C and held for 20 h. Following this annealing step, primary drying (at 50 to 60 mTorr) was carried out at a shelf temperature of −30°C for 30 h. Secondary drying was conducted, first at −10°C for 2 h, and then at 0 and +10°C each for 2 h. At the end of the cycle, the vials were capped with rubber stoppers (two-leg gray butyl, Fisher Scientific) under dry nitrogen gas purge and then stored in a refrigerator.

RESULTS AND DISCUSSION

Based on their XRD patterns, the 'as-received' trehalose was identified as the dihydrate, while sucrose, mannitol (β-) and glycine (α-) were anhydrous forms. In addition, the other expected physical forms of these compounds could be readily identified by their unique XRD peaks. Trehalose dihydrate ($C_{12}H_{22}O_{11}\cdot 2H_2O$) was characterized by peaks at 8.8° (10.10 Å), 15.3° (5.79 Å), 16.9° (5.24 Å), and 17.6° 2θ (5.04 Å). The α-, β-, and γ-polymorphic forms of glycine

were identified by their respective peaks at 30.2° (2.96 Å), 18.0° (4.92 Å), and 21.8° 2θ (4.07 Å). Similarly, unique peaks of anhydrous α- [13.7° (6.46 Å) and 17.3° (5.12 Å) 2θ], β- [14.6° (6.06 Å) and 16.8° (5.27 Å) 2θ], and δ- [9.7° (9.11 Å) and 24.6° (3.62 Å) 2θ] polymorphic forms of mannitol facilitated their identification in multi-component systems. Mannitol hemihydrate ($C_6H_{14}O_6 \cdot 0.5H_2O$) was identified by the peaks at 9.6° (4.95 Å), 16.5° (5.37 Å), 18.0° (4.92 Å) and 20.5° 2θ (4.33 Å) (37). The DSC heating curves of trehalose dihydrate, sucrose, mannitol (β-) and glycine (α-) were in excellent agreement with that reported earlier (37–41).

Characterization of Frozen Solutions

Trehalose and Mannitol

Low-Temperature XRD. Previous studies demonstrated annealing-induced crystallization of trehalose dihydrate in frozen solutions (20,21). Upon cooling a buffered (succinate) trehalose solution, there was a pronounced increase in the freeze-concentrate pH. This was attributed to the sequential crystallization of ice, buffer components and trehalose dihydrate. In other words, crystallized buffer components facilitated the crystallization of trehalose dihydrate, which in turn caused further crystallization of buffer components. When a solution containing only trehalose was cooled, hexagonal ice was the only crystalline phase. Trehalose dihydrate peaks were evident after annealing the seeded frozen solution. Thus, external seeding of the frozen solution accelerated trehalose crystallization. We recognize that during the freeze-drying process, external seeding is not a practical option. However, we hypothesize that the presence of a readily crystallizing solute, through *in situ* seeding, will substantially accelerate trehalose crystallization. To test this hypothesis, we investigated the influence of mannitol, a readily crystallizing solute.

Fig. 2 contains the XRD patterns of a frozen aqueous solution containing trehalose and mannitol recorded during annealing at −18°C. The eutectic melting temperatures of trehalose-water and mannitol-water binary systems are −2.5 and −1.5°C, respectively, and the glass transition temperature of trehalose freeze-concentrate is reported to be in the range of −32 to −40°C (42). Since maximum crystallization is expected at the midpoint between Te and Tg', annealing was conducted at −18°C (43). Soon after cooling to −40°C, hexagonal ice was the only crystallized phase (Fig. 2). However upon warming the solution to the annealing temperature (−18°C), mannitol readily crystallized as mannitol hemihydrate (Fig. 2). This assignment was based on the peaks at 9.6, 18.0 and 20.5° 2θ. The low intensity peak at 9.7° 2θ (Fig. 2), attributable to δ-mannitol, gradually merged with the hemihydrate peak at 9.6° 2θ.

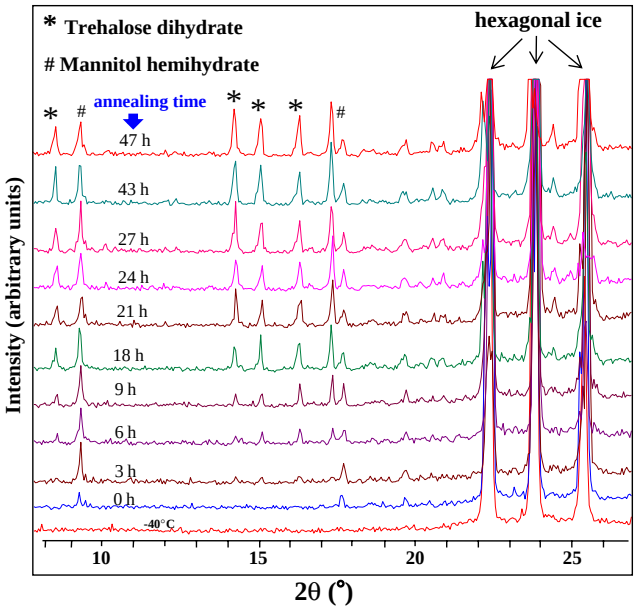

Fig. 2 XRD patterns of frozen aqueous solution containing trehalose (4% *w/v*) and mannitol (2% *w/v*) recorded during annealing. The solution was initially cooled from RT to −40°C and held for 15 min, and the XRD pattern was recorded (bottom pattern). The solution was then heated to −18°C and annealed for 47 h. The characteristic peaks of hexagonal ice, mannitol hemihydrate, and trehalose dihydrate are identified.

Hence, we conclude that the frozen matrix contains a mixture of anhydrous δ-mannitol (trace) and mannitol hemihydrate (dominant phase).

As the annealing progressed to 3 h, there was a considerable increase in mannitol hemihydrate peak intensities and concomitant appearance of trehalose dihydrate (peaks at 15.2° and 16.9° 2θ). Upon further annealing, the intensity of both mannitol hemihydrate and trehalose dihydrate peaks increased substantially, indicating a sequential crystallization of mannitol hemihydrate and trehalose dihydrate. The integrated intensities of the characteristic peaks, a quantitative measure of the crystallized phases, are plotted as a function of annealing time (Fig. 3). Upon annealing, mannitol hemihydrate peaks appeared readily, and those of trehalose dihydrate appeared after 3 h. In contrast, our previous study revealed that peaks of trehalose dihydrate appeared after 12 h of annealing the seeded frozen solutions but only after 3 days of annealing the unseeded system (20,21). Thus, when compared with external seeding, the presence of crystalline mannitol appeared to be more effective in promoting trehalose crystallization. Up to about 40 h of annealing, the peak intensities of mannitol hemihydrate and trehalose dihydrate showed a pronounced increase as a function of annealing time, and then leveled off.

To determine the crystallized fraction of trehalose in frozen solution, the XRD pattern of a physical mixture containing ~4.4 g of trehalose dihydrate and ~95.6 of

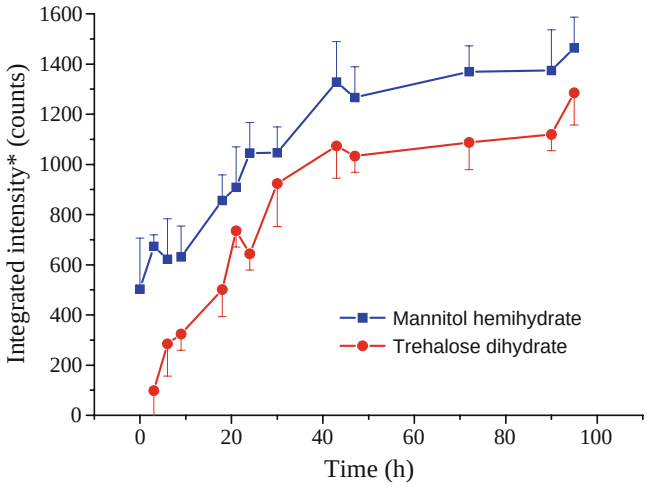

Fig. 3 Plot of the integrated intensities (mean ± SD; $n = 3$) of the characteristic peaks of mannitol hemihydrate and trehalose dihydrate as a function of annealing time. The solutions (4% *w/v* trehalose and 2% *w/v* mannitol) were first cooled from RT to −40°C, held for 15 min, and then warmed to −18°C. Note: Fig. 2 contains the XRD patterns from which the intensities were obtained. * Sum of the intensities of (i) the 9.8 and 17.8° 2θ peaks of mannitol hemihydrate, and (ii) the 9.0 and 24.9° 2θ peaks of trehalose dihydrate.

powder ice was recorded (data not shown). Based on the intensity of the trehalose dihydrate peaks, it was estimated that 40 to 50% of the trehalose had crystallized after annealing for 90 h.

Differential Scanning Calorimetry (DSC). Fig. 4 shows the DSC heating curve of frozen and annealed aqueous solution containing trehalose (4% *w/v*) and mannitol (2% *w/v*). During the initial cooling, only ice crystallization was evident (data not shown). However, when the annealed sample was rewarmed from −50°C to RT, two endotherms overlapped with ice melting (Fig. 4, inset). To deconvolute the overlapping thermal events, modulated DSC is typically utilized, wherein the 'reversible' (for e.g., melting or glass transition) and 'nonreversible' (for e.g., crystallization or degradation) thermal events are separated using a sinusoidal heating rate. However, modulated DSC is not very useful in separating overlapping reversible events such as melting endotherms of two components with close melting points (44).

In an effort to separate the overlapping melting events, Fourier self-deconvolution was utilized. It is typically used to deconvolute overlapping peaks in the FT-IR spectra of multi-component mixtures (45). However, its applicability and validity in the deconvolution of DSC heating curves has not been established. While a broad FT-IR peak can be a consequence of overlapping peaks, such an assumption in DSC heating curves can be erroneous. In DSC, peak broadening can be brought about by dissolved solutes. But in our frozen system (trehalose and mannitol), since the temperature range of interest was very close to the eutectic temperatures (trehalose dihydrate-ice and mannitol hemihydrates-ice), we assumed that any peak broadening due to the dissolved solute will be negligible. Therefore, the observed broadening was attributed to the overlapping eutectic melting events.

The deconvoluted DSC curve showed three melting events with onset temperatures of −2.3, −0.9 and 1.0°C. The sequence of the melting events can be postulated from the aqueous solubility of the individual components—the higher the solubility, the lower the eutectic temperature. The equilibrium aqueous solubility of mannitol is significantly lower than that of trehalose at all temperatures. For example, while the solubility of mannitol at 10°C is 0.08 M, that of trehalose is 1.48 M. At this temperature, for both these systems, the solid in contact with the saturated solution is the corresponding anhydrous form. However, our XRD work has unambiguously revealed that at temperatures <0°C, only the hydrate forms (dihydrate in case of trehalose and hemihydrate in case of mannitol) existed (Fig. 6). Therefore, the first two thermal events are respectively attributed to the eutectic melting of trehalose dihydrate-ice (−2.3°C) and mannitol hemihydrate-ice (−0.9°C) binary systems and the final endotherm to ice melting. To substantiate this assignment, aqueous solutions of trehalose and mannitol were individually subjected to DSC (Fig. 5 panels a & b). The binary eutectic temperatures of trehalose dihydrate-ice (panel a) and mannitol hemihydrate-ice (panel b) were −2.4 and −1.3°C,

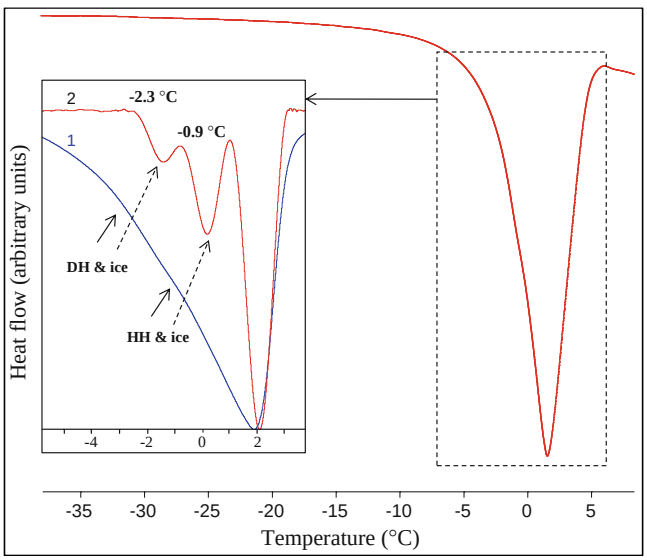

Fig. 4 DSC heating curve of frozen aqueous solution containing trehalose (4% *w/v*) and mannitol (2% *w/v*). The solution was cooled from RT to −50°C, held for 15 min, heated to −18°C, annealed for 24 h, cooled back to −50°C, and rewarmed to RT. The heating and cooling rate was 1°C/min. Only the final heating curve is shown. The thermal events of interest are shown in the inset. While curve 1 represents the heat flow, curve 2 is the Fourier self-deconvolution of curve 1. The melting (T_{onset}) of various crystalline phases is pointed out. DH: trehalose dihydrate; HH: mannitol hemihydrates.

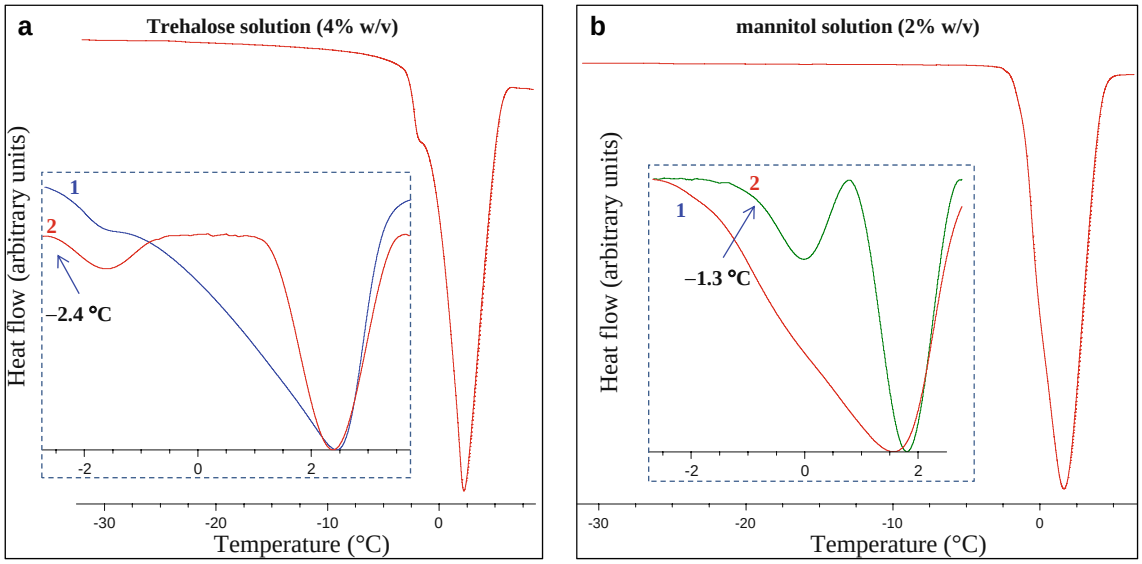

Fig. 5 DSC heating curves of frozen aqueous solution of **a**) trehalose and **b**) mannitol. The solutions were cooled from RT to −50°C, held for 15 min, heated to −18°C and annealed for 24 h, then cooled back to −50°C, and finally rewarmed to RT. The heating and cooling rate was 1°C/min. The thermal events of interest are shown in the inset. While curve 1 represents the heat flow, curve 2 represents the Fourier self-deconvolution of curve 1.

respectively (onset temperature). These were in excellent agreement with the reported temperatures of −2.5 (trehalose-ice) and −1.5°C (mannitol-ice) (9,46,47).

To interpret the thermal events observed in the DSC, similar experiments were performed using the diffractometer. The XRD patterns were recorded when the annealed solution was warmed (Fig. 6). As the temperature was progressively increased, the characteristic peaks of trehalose dihydrate and mannitol hemihydrate were evident up to −2°C (Fig. 6). However, when the temperature was increased from −2.0 to −1.0°C, both the peaks of trehalose dihydrate and mannitol hemihydrate disappeared simultaneously, but the ice peaks were observed up to 0°C. Thus, based on XRD, we cannot distinguish between trehalose-mannitol-water ternary eutectic system and trehalose-water and mannitol-water binary eutectic systems. This limitation of XRD comes about because the eutectic temperatures of the two binary systems are very close to each other. However, XRD revealed the identity of the crystalline phases in the system—something that cannot be obtained directly from DSC. Thus, using both DSC and XRD, the eutectic melting of trehalose dihydrate-ice and mannitol hemihydrate-ice could be established.

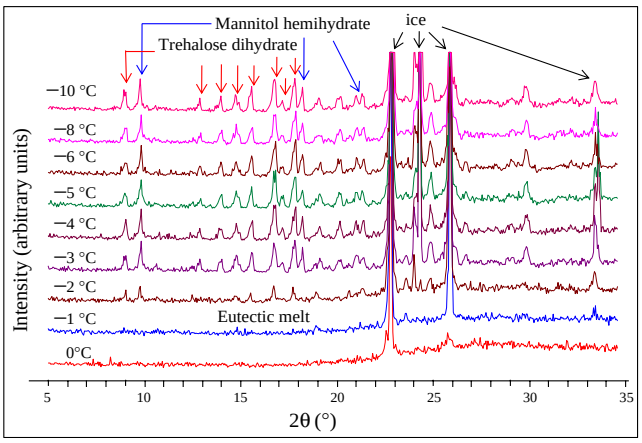

Fig. 6 XRD patterns of frozen aqueous solution containing trehalose (4% *w/v*) and mannitol (2% *w/v*) recorded during annealing. The solution was initially cooled from RT to −40°C, held for 15 min, heated to −18°C and annealed for 48 h and finally warmed to RT. The XRD patterns recorded during warming (−10 to 0°C; top to bottom) are shown. The characteristic peaks of hexagonal ice, mannitol hemihydrate, and trehalose dihydrate are designated by arrows.

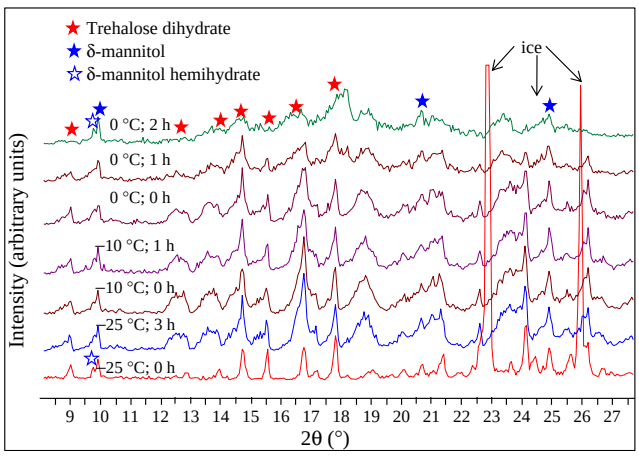

Fig. 7 The XRD patterns of the solution containing trehalose (4% *w/v*) and mannitol (2% *w/v*), recorded during the drying stage of lyophilization. The sample was first cooled from RT to −40 at 1°C/min, held for 15 min, heated to −18°C, and annealed for 24 h. The primary drying was conducted at −25°C for 3 h and the secondary drying, first at −10°C for 1 h and then at 0°C for 2 h. The characteristic peaks of ice, trehalose dihydrate and δ-mannitol are pointed out.

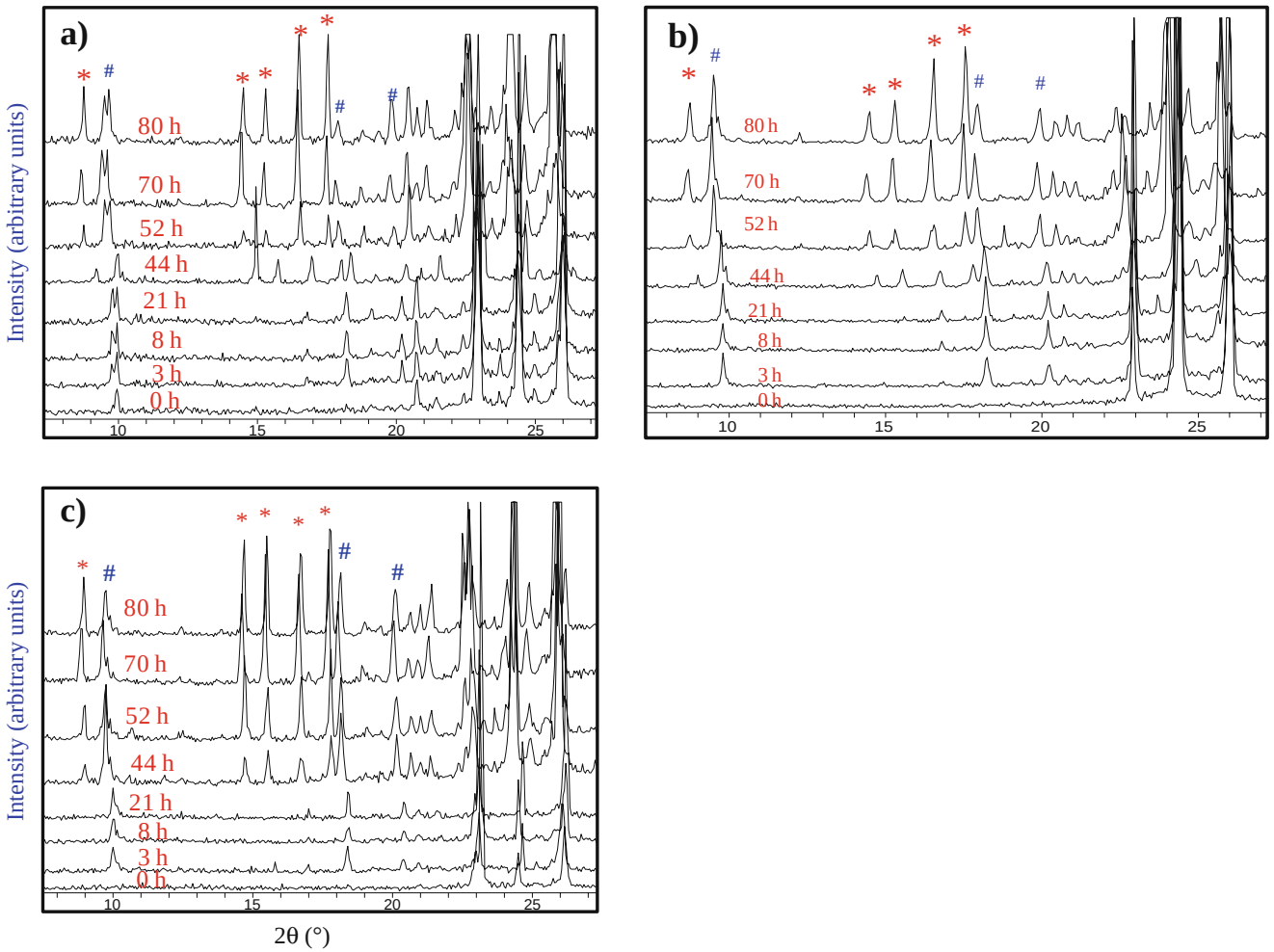

Fig. 8 Overlaid XRD patterns of frozen aqueous solution containing trehalose (4% *w/v*), mannitol (2% *w/v*), and model proteins, **a**) lysozyme, **b**) LDH; and **c**) catalase, recorded during annealing at −18°C. The samples were initially cooled from RT to −40, held for 15 min and then heated to −18°C. Both the heating and cooling rates were 1°C/min. The characteristic peaks of mannitol hemihydrate (#) and trehalose dihydrate (*) are pointed out.

In Situ Freeze-Drying XRD. Previous studies indicated that crystalline hydrates, for example, disodium succinate hexahydrate and trehalose dihydrate, dehydrate into the corresponding amorphous anhydrates during drying (13,20,21). To monitor the phase behavior of trehalose dihydrate during drying and to understand the influence of mannitol hemihydrate on the dehydration of trehalose dihydrate, the entire freeze-drying cycle was performed in the X-ray diffractometer.

Fig. 7 contains the XRD patterns recorded during primary drying of the frozen aqueous solution containing trehalose and mannitol. When the drying was initiated at −25°C, the characteristic peaks of trehalose dihydrate, anhydrous δ-mannitol and mannitol hemihydrate (trace) were evident. At the end of primary drying, reflected by the complete disappearance of ice, the peaks of trehalose dihydrate and mannitol phases were retained. An increase in the drying temperature to −10°C did not bring about any pronounced changes in the XRD pattern. However, when the temperature was increased to 0°C and the drying was continued for 2 h, there was a pronounced decrease in the trehalose dihydrate peak intensities, reflecting its conversion to an amorphous anhydrate. The final lyophile contained amorphous anhydrous trehalose and δ-mannitol.

Thus, both XRD and DSC provided evidence for the crystallization of trehalose dihydrate in frozen solutions. The freeze-drying, in the sample chamber of the XRD, revealed the dehydration of trehalose dihydrate to amorphous anhydrate. The final lyophiles contained δ-mannitol and traces of mannitol hemihydrate.

Trehalose, Mannitol, and Protein

While trehalose dihydrate crystallization in frozen solutions was accelerated by a crystallizing cosolute (mannitol), the influence of non-crystallizing APIs was studied using LDH, catalase, and lysozyme as model proteins. The prelyo

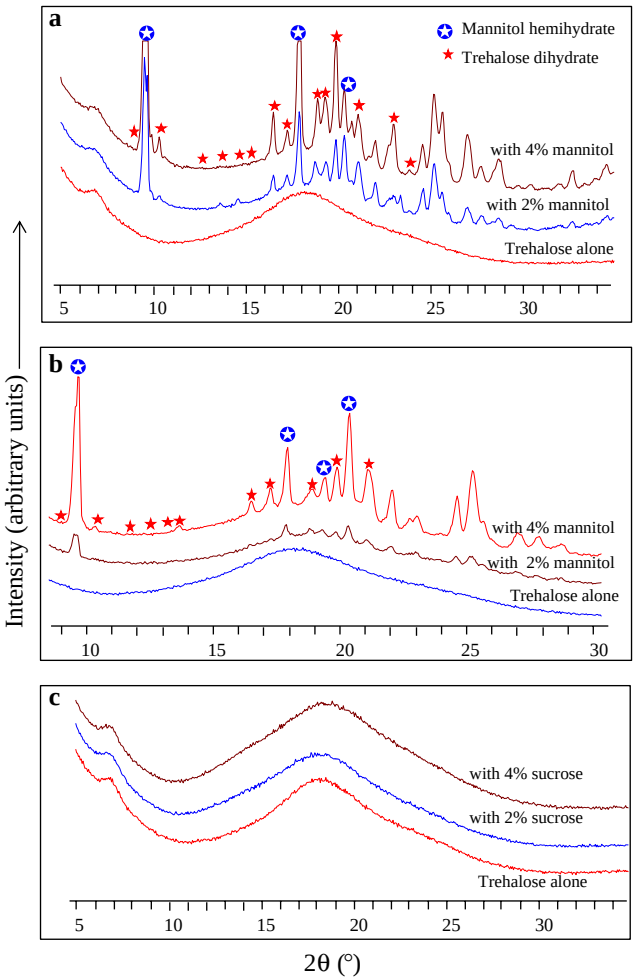

Fig. 9 XRD patterns of final lyophiles prepared from aqueous trehalose solutions containing either mannitol or sucrose. Panel **a**: 2% *w/v* trehalose; panels **b** & **c**: 4% *w/v* trehalose. The concentration (*w/v*) of cosolute in the prelyophilization solution is given above each XRD pattern. The characteristic peaks of trehalose dihydrate and mannitol hemihydrate are pointed out.

solution contained API (2 mg/ml), trehalose (4% *w/v*) and mannitol (2% *w/v*).

Low-Temperature XRD. Aqueous solutions containing trehalose, mannitol, and model protein were cooled from RT to −40°C, held for 15 min, and then annealed at −18°C (Fig. 8). During cooling, only crystallization of ice was observed (data not shown). In contrast to the earlier system, the characteristic peaks of mannitol hemihydrate were not immediately evident at −18°C. The XRD patterns recorded during annealing are shown in Fig. 8. The kinetics of mannitol hemihydrate crystallization depended on the model protein. In the case of lysozyme, the mannitol hemihydrate peaks were observed as soon as the annealing temperature was reached (Fig. 8 panel a), while in the frozen solutions containing LDH (Fig. 8 panel b) or catalase (Fig. 8 panel c), annealing for 3 h was required to discern hemihydrate crystallization. In all the systems, upon further annealing, there was a pronounced increase in the peak intensities. Based on the overlapping peaks at 9.6° and 9.7° 2θ, it is evident that mannitol crystallized as a mixture—predominantly the hemihydrate with traces of the δ-form. However, based on the pronounced intensity of the 9.7° 2θ peak in the presence of lysozyme, it appears that this protein facilitated the crystallization of δ-mannitol (Fig. 8 panel b).

We earlier observed that in the absence of an API, trehalose crystallized after 3 h of annealing (Fig. 2) (20,21). In the presence of a non-crystallizing solute (model protein), trehalose crystallization was delayed and occurred only after 21 h of annealing. In general, the peak intensities increased with annealing time, and the peaks were quite pronounced after 44 h of annealing. Thus, there was clear evidence of sequential crystallization of ice, mannitol hemihydrate and trehalose dihydrate. The crystallization of a lyoprotectant can have serious implications on protein stability. As expected, all the non-crystallizing solutes (model protein) retarded but did not prevent trehalose dihydrate crystallization.

The combination of mannitol and trehalose in a protein formulation is atypical. However, we hypothesized that a readily crystallizing excipient such as mannitol would facilitate trehalose crystallization. It would be interesting to study the influence of other crystallizing solutes such as glycine and buffer components. Similarly, the presence of other formulation components could also influence mannitol crystallization. For example, in the presence of Tween 80, crystallization of mannitol is enhanced (48).

Trehalose, Mannitol, and Sucrose

In an effort to inhibit trehalose crystallization in frozen solutions, the effect of sucrose, another commonly used lyoprotectant, was investigated. Sucrose is widely reported to be a non-crystallizing solute. However, based on XRD and spectroscopic analysis, Mathalouthi *et al.* reported short range order in concentrated sucrose solutions (36,49,50). Prelyophilization solutions containing trehalose (4% *w/v*) and varying concentrations (2, 4, and 8% *w/v*) of sucrose were cooled from RT to −40°C, held for 15 min, and warmed to the annealing temperature (−18°C). Even after annealing for 12 days, hexagonal ice was the only crystalline phase observed (data not shown). At all trehalose concentrations, neither sucrose nor trehalose crystallized (data not shown). Sucrose, by remaining amorphous, effectively prevented trehalose crystallization. We did not evaluate the influence of mannitol on trehalose–sucrose–water ternary systems. However, it has been reported that in the presence of either sucrose or trehalose, mannitol crystallization in the final lyophile was inhibited (46).

Characterization of Final Lyophiles

Fig. 9 contains the XRD patterns of the final lyophiles prepared from prelyophilization solutions containing trehalose and either mannitol or sucrose. When the prelyo solution containing trehalose alone was freeze-dried in the laboratory lyophilizer, the finished product was X-ray amorphous (Fig. 9 panel a). However in the presence of mannitol, trehalose dihydrate peaks were evident (panel a). The intensity of the trehalose dihydrate peaks was much higher when the mannitol concentration was increased from 2% to 4% *w/v*. Irrespective of initial mannitol concentration, mannitol hemihydrate was evident. While the existence of mannitol hemihydrate in the final lyophile was not surprising, the presence of trehalose dihydrate was intriguing (47,51,52). Earlier we demonstrated that during drying, dehydration of trehalose dihydrate resulted in a predominantly amorphous lyophile.

Based on XRD, the lyophile obtained from a trehalose solution (4% *w/v*) was amorphous (panel b), but in the presence of mannitol, contained crystalline trehalose dihydrate (panel b). There was an increase in the trehalose dihydrate peak intensities as the mannitol concentration was increased from 2% to 4% *w/v* (panel b).

The drying-induced dehydration of trehalose dihydrate yielded a predominantly amorphous anhydrate (20,21). The current study indicated that in the presence of mannitol, dehydration of trehalose dihydrate was not complete. This raises an interesting question: *Can the presence of cosolutes alter the kinetics of water removal?* Our data suggest that with an increase in the mannitol-to-trehalose ratio, there was an *increase* in the intensities of trehalose dihydrate peaks (Fig. 9 panels a and b). Hence, it would be interesting to study the effect of cosolutes on the drying-induced dehydration rates of various crystalline hydrates.

SIGNIFICANCE

Trehalose crystallization was facilitated in the presence of a crystallizing solute. While the amorphous API (model proteins) decelerated trehalose crystallization, it did not decrease the extent of trehalose crystallization at the end of annealing. However, sucrose, a non-crystallizing excipient, completely inhibited the crystallization of trehalose dihydrate in the frozen and freeze-dried systems. Even when there is substantial trehalose crystallization, only about half of the total trehalose crystallized in the frozen solution. Therefore, the fraction of trehalose remaining amorphous might be adequate to provide lyoprotection. While it was reported that annealing, by modifying the ice crystal morphology, may improve the process efficiency, our results indicate that annealing might induce undesirable excipient crystallization with potential implications on API stability (53). In such circumstances, it will be prudent to consider other lyoprotectants. While sucrose is another widely used lyoprotectant, recently, maltodextrin and inulin have been identified as potential candidates (54).

CONCLUSIONS

Crystallization of trehalose, as trehalose dihydrate, in frozen solutions and its subsequent phase transformations during drying was investigated. While a readily crystallizing cosolute, such as mannitol, facilitated trehalose crystallization, non-crystallizing solutes, such as model proteins, retarded its crystallization. Sucrose, a non-crystallizing solute, completely inhibited trehalose crystallization during all the stages of freeze-drying.

ACKNOWLEDGEMENTS

We thank Dr Len Thomas and Dr Steve Aubuchon from TA instruments for their comments. The XRD work was carried out at the College of Science and Engineering Characterization Facility, University of Minnesota, which receives partial support from NSF through the MRSEC program.

REFERENCES

1. Pikal MJ. Freeze drying. In: Swarbrick J, editor. Encyclopedia of pharmaceutical technology, vol. 1. New York: Informa Healthcare; 2007. p. 1807–33.
2. Akers MJ, Vasudevan V, Stickelmeyer M. Formulation development of protein dosage forms. Pharm Biotechnol. 2002;14:47–127.
3. Carpenter JF, Pikal MJ, Chang BS, Randolph TW. Rational design of stable lyophilized protein formulations: some practical advice. Pharm Res. 1997;14:969–75.
4. Randolph TW. Phase separation of excipients during lyophilization: effects on protein stability. J Pharm Sci. 1997;86:1198–203.
5. Varshney DB, Kumar S, Shalaev EY, Sundaramurthi P, Kang S-W, Gatlin LA, *et al.* Glycine crystallization in frozen and freeze-dried systems: effect of pH and buffer concentration. Pharm Res. 2007;24:593–604.
6. Varshney DB, Sundaramurthi P, Kumar S, Shalaev EY, Kang S-W, Gatlin LA, *et al.* Phase transitions in frozen systems and during freeze-drying: quantification using synchrotron X-ray diffractometry. Pharm Res. 2009;26:1596–606.
7. Chatterjee K, Shalaev EY, Suryanarayanan R. Partially crystalline systems in lyophilization: II. Withstanding collapse at high primary drying temperatures and impact on protein activity recovery. J Pharm Sci. 2005;94:809–20.
8. Chatterjee K, Shalaev EY, Suryanarayanan R. Partially crystalline systems in lyophilization: I. Use of ternary state diagrams to determine extent of crystallization of bulking agent. J Pharm Sci. 2005;94:798–808.
9. Johnson RE, Kirchhoff CF, Gaud HT. Mannitol-sucrose mixtures —versatile formulations for protein lyophilization. J Pharm Sci. 2002;91:914–22.

10. Wang DQ, Hey JM, Nail SL. Effect of collapse on the stability of freeze-dried recombinant factor VIII and α-amylase. J Pharm Sci. 2004;93:1253–63.
11. Tang X, Pikal MJ. Design of freeze-drying processes for pharmaceuticals: Practical advice. Pharm Res. 2004;21:191–200.
12. Sundaramurthi P, Shalaev E, Suryanarayanan R. "pH Swing" in frozen solutions-consequence of sequential crystallization of buffer components. J Phys Chem Lett. 2010;1:265–8.
13. Sundaramurthi P, Shalaev E, Suryanarayanan R. Calorimetric and diffractometric evidence for the sequential crystallization of buffer components and consequent pH swing in frozen solutions. J Phys Chem B. 2010;114:4915–23.
14. Shalaev EY. The impact of buffer on processing and stability of freeze-dried dosage forms, part 1: solution freezing behavior. Am Pharm Rev. 2005;8:80–7.
15. van den Berg L. pH changes in buffers and foods during freezing and subsequent storage. Cryobiol. 1966;3:236–42.
16. Izutsu K, Yoshioka S, Takeda Y. The effects of additives on the stability of freeze-dried beta-galactosidase stored at elevated temperature. Int J Pharm. 1991;71:137–46.
17. Izutsu K, Yoshioka S, Terao T. Decreased protein-stabilizing effects of cryoprotectants due to crystallization. Pharm Res. 1993;10:1232–7.
18. Gomez G, Pikal MJ, Rodriguez-Hornedo N. Effect of initial buffer composition on pH changes during far-from-equilibrium freezing of sodium phosphate buffer solutions. Pharm Res. 2001;18:90–7.
19. Pikal-Cleland KA, Cleland JL, Anchordoquy TJ, Carpenter JF. Effect of glycine on pH changes and protein stability during freeze-thawing in phosphate buffer systems. J Pharm Sci. 2002;91:1969–79.
20. Sundaramurthi P, Suryanarayanan R. Trehalose crystallization during freeze-drying: implications on lyoprotection. J Phys Chem Lett. 2010;1:510–4.
21. Sundaramurthi P, Patapoff TW, Suryanarayanan R. Crystallization of trehalose in the frozen solutions and its phase behavior during drying. Pharm Res. doi:10.1007/s11095-010-0243-2
22. Davidson P, Sun WQ. Effect of sucrose/raffinose mass ratios on the stability of co-lyophilized protein during storage above the Tg. Pharm Res. 2001;18:474–9.
23. Kajiwara K, Franks F, Echlin P, Greer AL. Structural and dynamic properties of crystalline and amorphous phases in raffinose-water mixtures. Pharm Res. 1999;16:1441–8.
24. Kajiwara K, Motegi A, Sugie M, Franks F, Munekawa S, Igarashi T, *et al.* Studies on raffinose hydrates. In: Levine H, editor. Amorphous food and pharmaceutical systems. Cambridge: Royal Society of Chemistry; 2002. p. 121–30.
25. Saleki-Gerhardt A, Stowell JG, Byrn SR, Zografi G. Hydration and dehydration of crystalline and amorphous forms of raffinose. J Pharm Sci. 1995;84:318–23.
26. Bennett AN, Ness AR. Viscosity of beet house sirups. Ind Eng Chem. 1930;22:91–6.
27. Miller DP, De Pablo JJ. Calorimetric solution properties of simple saccharides and their significance for the stabilization of biological structure and function. J Phys Chem B. 2000;104: 8876–83.
28. Szkudlarek BA. Selective crystallization of phosphate buffer components and pH changes during freezing: Implications to protein stability, PhD Thesis, Department of Pharmaceutics, University of Michigan, Ann Arbor, 1997, pp 188.
29. Jeffrey GA, Kim HS. Conformations of the alditols. Carbohydr Res. 1970;14:207–16.
30. Jeffrey GA, Takagi S. Hydrogen-bond structure in carbohydrate crystals. Acc Chem Res. 1978;11:264–70.
31. Jeffrey GA. Intramolecular hydrogen-bonding in carbohydrate crystal structure. Carbohydr Res. 1973;28:233–41.
32. Sundaralingam M. Some aspects of stereochemistry and hydrogen bonding of carbohydrates related to polysaccharide conformations. Biopolymers. 1968;6:189–213.
33. Berman HM. The crystal structure of a trisaccharide, raffinose pentahydrate. Acta Crystallogr. 1970;B26:290–9.
34. Brown GM, Levy HA. Sucrose: Precise determination of crystal and molecular structure by neutron diffraction. Science. 1962;141:921–3.
35. Brown GM, Rohrer DC, Berking B, Beevers CA, Gould RO, Simpson R. The crystal structure of α, α-trehalose dihydrate from three independent X-ray determinations. Acta Crystallogr. 1972; B28:3145–58.
36. Mathlouthi M. X-ray diffraction study of the molecular association in aqueous solutions of D-fructose, D-glucose, and sucrose. Carbohydr Res. 1981;91:113–23.
37. Powder Diffraction File. Hexagonal ice, card # 00-042-1142; D-trehalose dihydrate, card # 00-029-1955; trehalose anhydrate, card # 00-003-0312; β-succinic acid, card # 00-031-1899; α-succinic acid, card # 00-031-1898; monosodium succinate, card # 00-030-1927; sucrose, card # 00-024-1977; β-D-mannitol, card # 00-022-1797; δ-D-mannitol, card # 00-022-1794. International Centre for Diffraction Data, Newtown Square, PA; 2004.
38. Pyne A, Chatterjee K, Suryanarayanan R. Solute crystallization in mannitol-glycine systems—implications on protein stabilization in freeze-dried formulations. J Pharm Sci. 2003;92:2272–83.
39. Pyne A, Suryanarayanan R. Phase transitions of glycine in frozen aqueous solutions and during freeze-drying. Pharm Res. 2001;18:1448–54.
40. Surana R, Pyne A, Suryanarayanan R. Effect of aging on the physical properties of amorphous trehalose. Pharm Res. 2004;21:867–74.
41. Surana R, Pyne A, Suryanarayanan R. Effect of preparation method on physical properties of amorphous trehalose. Pharm Res. 2004;21:1167–76.
42. Chang BS, Randall CS. Use of subambient thermal analysis to optimize protein lyophilization. Cryobiology. 1992;29:632–56.
43. Mullin JW, editor. Crystallization. 4th ed. Burlington: Elsevier Butterworth-Heinemann; 2001.
44. Gill PS, Sauerbrunn SR, Reading M. Modulated differential scanning calorimetry. J Themal Anal. 1993;40:931–9.
45. McClure WF, Davies AMC. Fourier self-deconvolution in the analysis of near infrared spectra of chemically complex samples. Mikrochim Acta. 1988;1:93–6.
46. Kim AI, Akers MJ, Nail SL. The physical state of mannitol after freeze-drying: effects of mannitol concentration, freezing rate, and a noncrystallizing cosolute. J Pharm Sci. 1998;87:931–5.
47. Liao X, Krishnamurthy R, Suryanarayanan R. Influence of the active pharmaceutical ingredient concentration on the physical state of mannitol—implications in freeze-drying. Pharm Res. 2005;22:1978–85.
48. Haikala R, Eerola R, Tanninen VP, Yliruusi J. Polymorphic changes of mannitol during freeze-drying: effect of surface-active agents. PDA J Pharm Sci Technol. 1997;51:96–101.
49. Mathlouthi M, Cholli AL, Koenig JL. Spectroscopic study of the structure of sucrose in the amorphous state and in aqueous solution. Carbohydr Res. 1986;147:1–9.
50. Mathlouthi M, Luu C, Mefroy-Bigot AM, Luu DV. Laser-Raman study of solute-solvent interactions in aqueous solutions of D-fructose, D-glucose, and sucrose. Carbohydr Res. 1980;81:213–23.
51. Liao X, Krishnamurthy R, Suryanarayanan R. Influence of processing conditions on the physical state of mannitol—implications in freeze-drying. Pharm Res. 2007;24:370–6.
52. Lu X, Pikal MJ. Freeze-drying of mannitol-trehalose-sodium chloride-based formulations: the impact of annealing on dry layer resistance to mass transfer and cake structure. Pharm Dev Technol. 2004;9:85–95.
53. Searles JA, Carpenter JF, Randolph TW. Annealing to optimize the primary drying rate, reduce freezing-induced drying rate heterogeneity, and determine Tg' in pharmaceutical lyophilization. J Pharm Sci. 2001;90:872–87.
54. Corveleyn S, Remon J-P. Maltodextrins as lyoprotectants in the lyophilization of a model protein, LDH. Pharm Res. 1996;13:146–50.